Meccanica (2013) 48:2577–2583
DOI 10.1007/s11012-013-9787-7

BRIEF NOTES AND DISCUSSIONS

Newtonian flow in a triangular duct with slip at the wall

Georgios C. Georgiou · George Kaoullas

Received: 18 December 2012 / Accepted: 8 July 2013 / Published online: 2 August 2013
© Springer Science+Business Media Dordrecht 2013

Abstract We consider the Newtonian Poiseuille flow in a tube whose cross-section is an equilateral triangle. It is assumed that boundary slip occurs only above a critical value of the wall shear stress, namely the slip yield stress. It turns out that there are three flow regimes defined by two critical values of the pressure gradient. Below the first critical value, the fluid sticks everywhere and the classical no-slip solution is recovered. In an intermediate regime the fluid slips only around the middle of each boundary side and the flow problem is not amenable to analytical solution. Above the second critical pressure gradient non-uniform slip occurs everywhere at the wall. An analytical solution is derived for this case and the results are discussed.

Keywords Poiseuille flow · Newtonian fluid · Slip · Slip yield stress · Triangular duct

G.C. Georgiou (✉)
Department of Mathematics and Statistics,
University of Cyprus, P.O. Box 20537, 1678 Nicosia,
Cyprus
e-mail: georgios@ucy.ac.cy

G. Kaoullas
Oceanography Center, University of Cyprus,
P.O. Box 20537, 1678 Nicosia, Cyprus

1 Introduction

Slip at the wall occurs in a variety of macroscopic flows of industrial interest, such as in flows of polymer melts and suspensions, leading to many interesting phenomena and instabilities. For example, it is well-established that slip combined with compressibility leads to the so-called stick-slip polymer extrusion instability [1]. Slip effects are also very important in microfluidic applications [2]. Two recent reviews on wall slip are those of Neto et al. for Newtonian liquids [3] and of Hatzikiriakos for molten polymers [4].

In his review paper on the subject, Denn [1] notes that the experimental data show that the slip velocity is in general a function of the wall shear stress, the wall normal stress (which includes pressure), the temperature, the molecular weight and its distribution, and the fluid/wall interface, e.g. the interaction between the fluid and the solid surface and surface roughness. Navier [5] proposed a simple slip law relating the wall shear stress, τ_w, to the slip velocity, u_w, defined as the velocity of the fluid relative to that of the wall:

$$\tau_w = \beta u_w \tag{1}$$

where β is the slip coefficient, which varies in general with temperature, normal stress and pressure, molecular parameters, and the characteristics of the fluid/wall interface. The two limiting cases of no slip and perfect slip are obtained for $\beta \to \infty$ and $\beta = 0$, respectively. The slip coefficient is related to the extrapolation length, b, which is defined as the characteristic

length equal to the distance that the velocity profile at the wall must be extrapolated to reach zero, by means of

$$\beta \equiv \frac{\eta}{b} \tag{2}$$

where η is the viscosity.

Many different extensions of Navier's law have been proposed, the most important of which the generalizations to power-law and dynamic slip equations. The reader is referred to the recent review of Hatzikiriakos [4] for more details. In the present work, we are interested in models allowing slip only above a certain critical value of wall shear stress, the slip yield stress, τ_c, as suggested by experimental data on several fluid systems (see [6, 7] and references therein). In his review, Sochi [6] notes that the slip yield stress characterizes the fluid-solid system and the existing physical conditions. A simple extension of Navier's law to include slip yield stress is the following

$$\begin{cases} u_w = 0, & \tau_w \le \tau_c \\ \tau_w = \tau_c + \beta u_w, & \tau_w > \tau_c \end{cases} \tag{3}$$

The above slip model was first proposed for Newtonian fluid flow by Spikes and Granick [8] who tested its applicability on experimental data and discussed its possible physical mechanisms. The extension of the above model with the introduction of a power-law exponent is very often used for (non-Newtonian) pastes and colloidal suspensions [9, 10].

Ebert and Sparrow [11] derived analytical solutions of steady-state Newtonian Poiseuille flows with Navier slip in rectangular and annular ducts. It was only recently that analytical solutions for time-dependent and periodic flows with Navier slip have been published, namely by Majdalani [12], Wu et al. [13], and Wiwatanapataphee et al. [14] for the plane, round, and annular flows, respectively. A brief review of exact steady-state solutions for slip flow in ducts and channels has been recently published by Wang [15].

Wang [16] presented a rare close form solution for the steady-state Newtonian Poiseuille flow in a tube, whose cross-section is an equilateral triangle, assuming that Navier slip occurs along the wall. He also pointed out that exact solutions for other polygons do not exist. The objective of the present work is to extend his solution and analysis to the case of slip with non-zero slip yield stress. Such solutions for steady pressure-driven flows in other geometries, i.e. planar, axisymmetric, annular, and rectangular Poiseuille flows have been recently presented in [17].

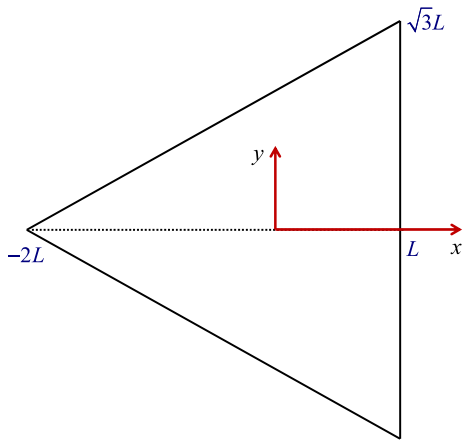

Fig. 1 Cross-section of the duct and coordinate system

2 Governing equations

The pressure-driven flow of a Newtonian liquid in a triangular duct, the cross-section of which is a equilateral triangle is considered. Each side has a length of $2\sqrt{3}L$ and the origin of the Cartesian coordinates (x, y) is taken at the center of the triangle, as illustrated in Fig. 1. The flow is assumed steady, creeping and incompressible and gravity is neglected. Under these assumptions, the flow is unidirectional and the z-velocity component, u, satisfies the Poisson equation

$$\frac{\partial^2 u}{\partial x^2} + \frac{\partial^2 u}{\partial y^2} = -\frac{1}{\eta}\left(-\frac{\partial p}{\partial z}\right) \tag{4}$$

where $(-\partial p/\partial z)$ is the pressure gradient.

As for the boundary condition at the duct walls, it is assumed that slip occurs following the slip Eq. (3). Along the wall $x = L$ (Fig. 1) the wall shear stress is:

$$\tau_w = |\tau_{zx}|_{x=L} = -\eta \left.\frac{\partial u}{\partial x}\right|_{x=L} \tag{5}$$

and therefore in the case of slip ($\tau_w > \tau_c$) the boundary condition (3) becomes

$$-\eta \left.\frac{\partial u}{\partial x}\right|_{x=L} = \tau_c + \beta u|_{x=L} \tag{6}$$

3 The exact solution

Wang [16] noted that a threefold symmetrical solution to Eq. (4) is given as

$$u = c_1 - \frac{1}{4\eta}\left(-\frac{\partial p}{\partial z}\right)\left[c_2\cos(3\theta)r^3 + r^2\right] \tag{7}$$

where the cylindrical polar coordinates (r,θ) are centered at the middle of the duct and c_1 and c_2 are positive constants determined by the boundary conditions. In Cartesian coordinates (Fig. 1), this solution takes the form

$$u = c_1 + \frac{1}{4\eta}\left(-\frac{\partial p}{\partial z}\right)\left[c_2\left(3xy^2 - x^3\right) - x^2 - y^2\right] \tag{8}$$

Following Wang [16] we demand that the constants c_1 and c_2 are such that the slip condition is satisfied along the side $x = L$. It is easy to see that both the slip velocity and the wall shear stress are parabolas:

$$u_w = c_1 - \frac{1}{4\eta}\left(-\frac{\partial p}{\partial z}\right)\left[(1 + c_2L)L^2 + (1 - 3c_2L)y^2\right] \tag{9}$$

and

$$\tau_w = \frac{1}{4}\left(-\frac{\partial p}{\partial z}\right)\left[(2 + 3c_2L)L - 3c_2y^2\right] \tag{10}$$

The no-slip regime The well-known no-slip solution is considered here in order to derive the critical pressure-gradient below which $\tau_w \le \tau_c$. By demanding that the velocity vanishes everywhere at the wall, one gets from Eq. (9):

$$c_1 = \frac{1}{3\eta}\left(-\frac{\partial p}{\partial z}\right)L^2 \quad \text{and} \quad c_2 = \frac{1}{3L}$$

Therefore in the case of no-slip

$$u = \frac{1}{12\eta}\left(-\frac{\partial p}{\partial z}\right)L^2\left[4 + \frac{1}{L^3}\left(3xy^2 - x^3\right) - 3\left(x^2 + y^2\right)\right] \tag{11}$$

and

$$\tau_w = \frac{1}{4}\left(-\frac{\partial p}{\partial z}\right)L\left(3 - \frac{y^2}{L^2}\right) \tag{12}$$

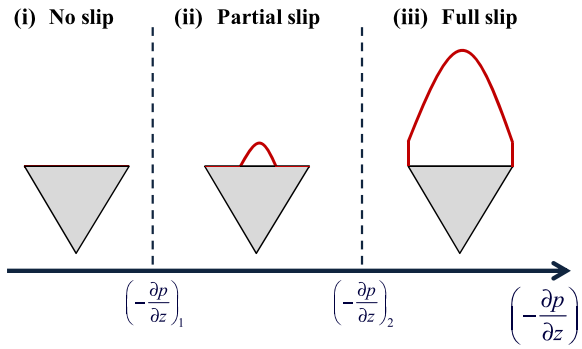

Fig. 2 Sketch showing the three different possibilities in the case of non-zero slip yield stress

The wall shear stress attains its maximum at the middle of the side:

$$\tau_{w,max} = \frac{3}{4}\left(-\frac{\partial p}{\partial z}\right)L \tag{13}$$

In the case of a slip equation with non-zero slip yield stress, the critical pressure below which no slip occurs corresponds to $\tau_{w,max} = \tau_c$, which gives

$$\left(-\frac{\partial p}{\partial z}\right)_1 = \frac{4\tau_c}{3L} \tag{14}$$

The solution in the case of slip Let us now consider the case where slip occurs along the side $x = L$. From Eq. (10) we note that the maximum and minimum wall shear stresses are respectively at the middle of a side and the vertices:

$$\tau_{w,max} = \frac{1}{4}\left(-\frac{\partial p}{\partial z}\right)L(2 + 3c_2L) \tag{15}$$

and

$$\tau_{w,min} = \frac{1}{2}\left(-\frac{\partial p}{\partial z}\right)L(1 - 3c_2L) \tag{16}$$

It is clear that if $\tau_{w,min} \le \tau_c < \tau_{w,max}$, slip does occur but only in the central part of a side. If $\tau_{w,min} > \tau_c$, slip occurs everywhere along the side. The critical pressure for this to happen is

$$\left(-\frac{\partial p}{\partial z}\right)_2 = \frac{2\tau_c}{L(1 - 3c_2L)} \tag{17}$$

Therefore, we have three flow regimes, illustrated in the sketch of Fig. 2:

(i) For $(-\partial p/\partial z) \le (-\partial p/\partial z)_1$, no slip occurs; the velocity and wall shear stress are given by Eqs. (10) and (11), respectively.
(ii) For $(-\partial p/\partial z)_1 < (-\partial p/\partial z) \le (-\partial p/\partial z)_2$, slip does occur but only in the central part of a boundary side.
(iii) For $(-\partial p/\partial z) > (-\partial p/\partial z)_2$, slip occurs everywhere along the side.

It should be noted that no exact solution is possible in case (ii) due to the non-linearity of the boundary condition. The solution for flow regime (iii) is easily derived as in Wang [16]. Substituting Eqs. (9) and (10) into Eq. (3) and setting the coefficients of powers of y to zero yields

$$c_1 = \frac{1}{6\eta}\left(-\frac{\partial p}{\partial z}\right)L^2\frac{(2+6B+3B^2)}{(1+B)} - \frac{\tau_c}{\beta} \quad \text{and}$$

$$c_2 = \frac{1}{3L(1+B)}$$

where

$$B \equiv \frac{\eta}{\beta L} \tag{18}$$

is the dimensionless slip number. Substituting c_2 into Eq. (17), one gets:

$$\left(-\frac{\partial p}{\partial z}\right)_2 = \frac{2\tau_c(1+B)}{LB} \tag{19}$$

Hence, when $(-\partial p/\partial z) > (-\partial p/\partial z)_2$ the velocity is given by

$$u = \frac{1}{12\eta}\left(-\frac{\partial p}{\partial z}\right)\frac{L^2}{1+B}\left[4+12B+6B^2 + \frac{1}{L^3}\left(3xy^2-x^3\right) - \frac{3(1+B)}{L^2}\left(x^2+y^2\right)\right] - \frac{\tau_c}{\beta} \tag{20}$$

The solution for case (i), i.e. when $(-\partial p/\partial z) \le (-\partial p/\partial z)_1$, is recovered by setting $B=0$ and $\tau_c = 0$ (no slip), while the solution for $\tau_c = 0$ (Navier slip) is:

$$u = \frac{1}{12\eta}\left(-\frac{\partial p}{\partial z}\right)\frac{L^2}{1+B}\left[4+12B+6B^2 + \frac{1}{L^3}\left(3xy^2-x^3\right) - \frac{3(1+B)}{L^2}\left(x^2+y^2\right)\right] \tag{21}$$

The wall shear stress is independent of the slip yield stress:

$$\tau_w = \frac{1}{4}\left(-\frac{\partial p}{\partial z}\right)\frac{L}{1+B}\left(3+2B-\frac{y^2}{L^2}\right) \tag{22}$$

The volumetric flow rate is given by

$$Q = \frac{3\sqrt{3}}{20\eta}\left(-\frac{\partial p}{\partial z}\right)\frac{L^4}{1+B}\left(3+15B+10B^2\right) - \frac{3\sqrt{3}L^2\tau_c}{\beta} \tag{23}$$

4 Discussion

To facilitate our discussion we dedimensionalize the above solution scaling lengths by L, the pressure by τ_c, and the velocity by $\tau_c L/\eta$, and using stars to denote the dimensionless variables. It turns out that the dimensionless critical pressure gradients are:

$$\left(-\frac{\partial p}{\partial z}\right)_1^* = \frac{4}{3} \tag{24}$$

and

$$\left(-\frac{\partial p}{\partial z}\right)_2^* = 2+\frac{2}{B} \tag{25}$$

For the dimensionless velocity and the volumetric flow rate per area unit we have

$$u^* = \begin{cases} \frac{1}{12}\left(-\frac{\partial p}{\partial z}\right)^*[4+3x^*y^{*2}-x^{*3} \\ \quad -3(x^{*2}+y^{*2})], \quad \left(-\frac{\partial p}{\partial z}\right)^* < \frac{4}{3} \\ \frac{1}{12}\left(-\frac{\partial p}{\partial z}\right)^*\frac{1}{1+B}[4+12B+6B^2 \\ \quad +3x^*y^{*2}-x^{*3} \\ \quad -3(1+B)(x^{*2}+y^{*2})]-B, \\ \quad \left(-\frac{\partial p}{\partial z}\right)^* \ge 2+\frac{2}{B} \end{cases} \tag{26}$$

and

$$Q^* = \begin{cases} \frac{3}{20}\left(-\frac{\partial p}{\partial z}\right)^*, \quad \left(-\frac{\partial p}{\partial z}\right)^* < \frac{4}{3} \\ \frac{1}{20}\left(-\frac{\partial p}{\partial z}\right)^*\frac{(3+15B+10B^2)}{1+B} - B, \\ \quad \left(-\frac{\partial p}{\partial z}\right)^* \ge 2+\frac{2}{B} \end{cases} \tag{27}$$

In Fig. 3, we plotted the dimensionless volumetric flow rate for different values of the slip number. The lower

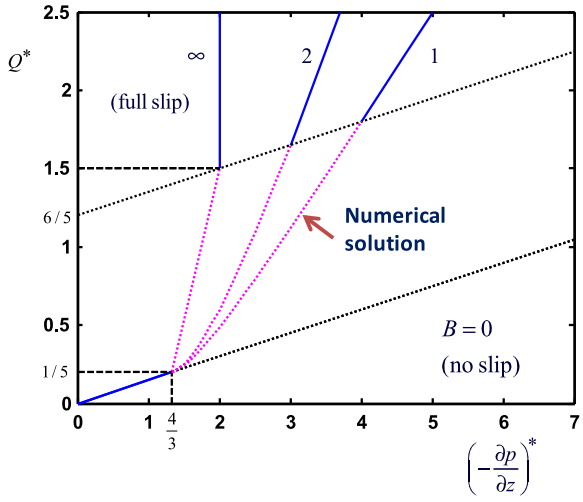

Fig. 3 Volumetric flow rate for different slip numbers (non-zero slip yield stress)

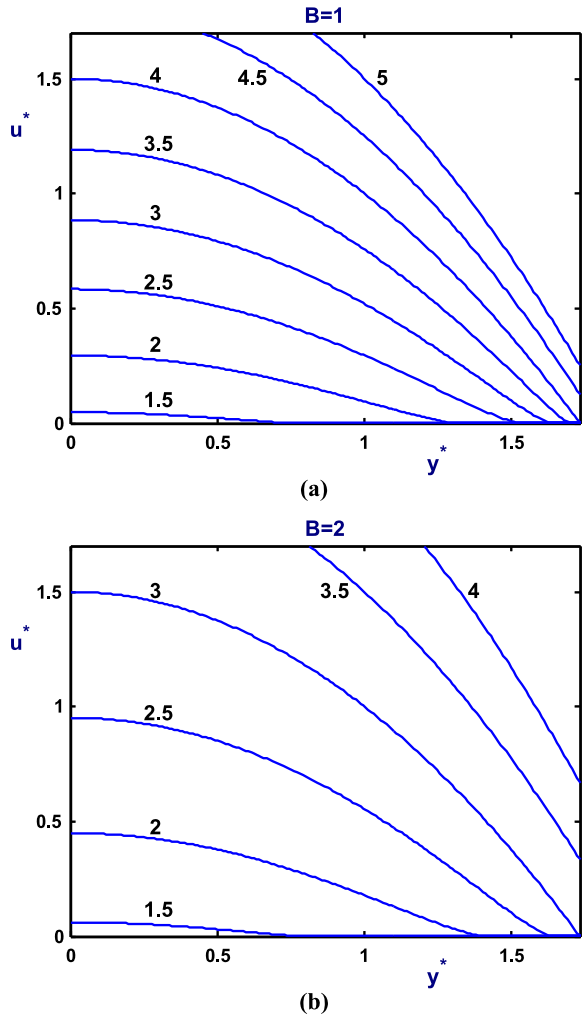

Fig. 4 The slip velocity along $x^* = 1$ for different values of the dimensionless pressure gradient: (**a**) $B = 1$ with $(-\partial p/\partial z)_2^* = 4$; (**b**) $B = 2$ with $(-\partial p/\partial z)_2^* = 3$

branch corresponds to the no-slip regime, which is independent of the slip number. The upper branch of the solution changes with the slip number; it is shifted to the left with an increasing slope as B increases. The intermediate dashed lines correspond to the case (ii) for which there is no analytical solution. These have been calculated numerically, i.e. using standard finite elements with a regularized version of the slip equation. Figure 4 shows the development of the slip velocity along $x^* = 1$ as the dimensionless pressure gradient is increased for the two slip numbers considered in Fig. 3, i.e. $B = 1$ and 2, for which $(-\partial p/\partial z)_2^* = 4$ and 3, respectively. One observes that the slip velocity at $(-\partial p/\partial z)_2^*$ is independent of B. It is easily verified from Eqs. (25) and (26) that $u_w(y^*) = (3 - y^{*2})/2$.

In Figs. 5 and 6, we plotted the analytical velocity contours at different values of the dimensionless pressure gradient for $B = 1$ and 10, respectively. The first two plots in each case correspond to the two critical pressure gradients. (Note that the magnitude of the velocity increases with the pressure gradient.) We observe that as the slip number increases the contours tend to become circular. This is also shown in Fig. 7, where we plotted the velocity contours for different values of B at the second critical pressure.

5 Conclusions

We have considered the Newtonian Poiseuille flow in a triangular duct assuming that slip occurs along the wall following a Navier-type slip law with a non-zero slip yield stress. It has been shown that there are three distinct flow regimes defined by two critical values of the imposed pressure-gradient. The first critical value depends solely on the slip yield stress, while the second one depends also on the slip coefficient. Below the first critical value, the fluid sticks everywhere at the duct walls and the well known no-slip solution applies. For pressure gradients greater than the second critical value, non-uniform slip occurs everywhere along the walls, which allows the derivation of an analytical solution, extending the solution of Wang [16] for Navier slip (zero slip yield stress). In the intermediate regime, there is no analytical solution. Solving numerically the

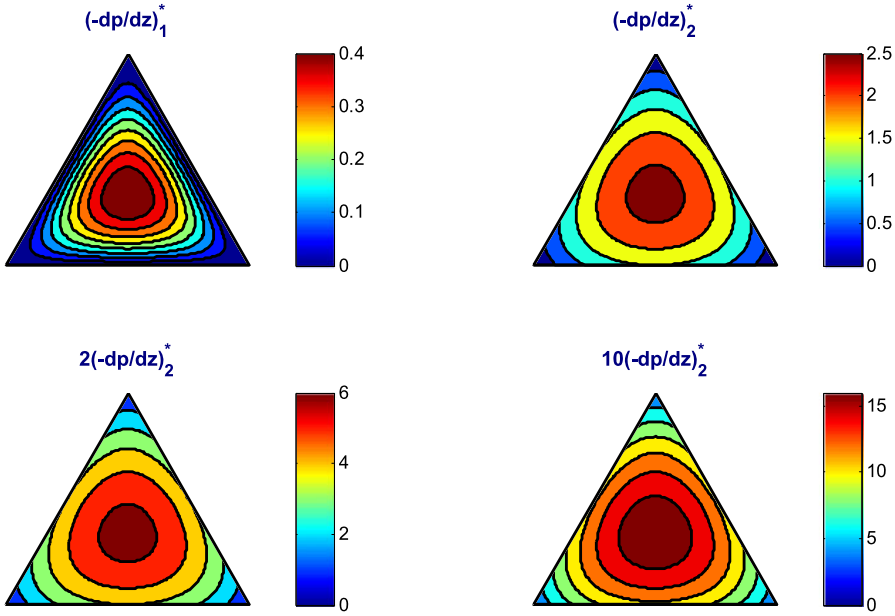

Fig. 5 Velocity contours for $B = 1$ and different values of the dimensionless pressure gradient

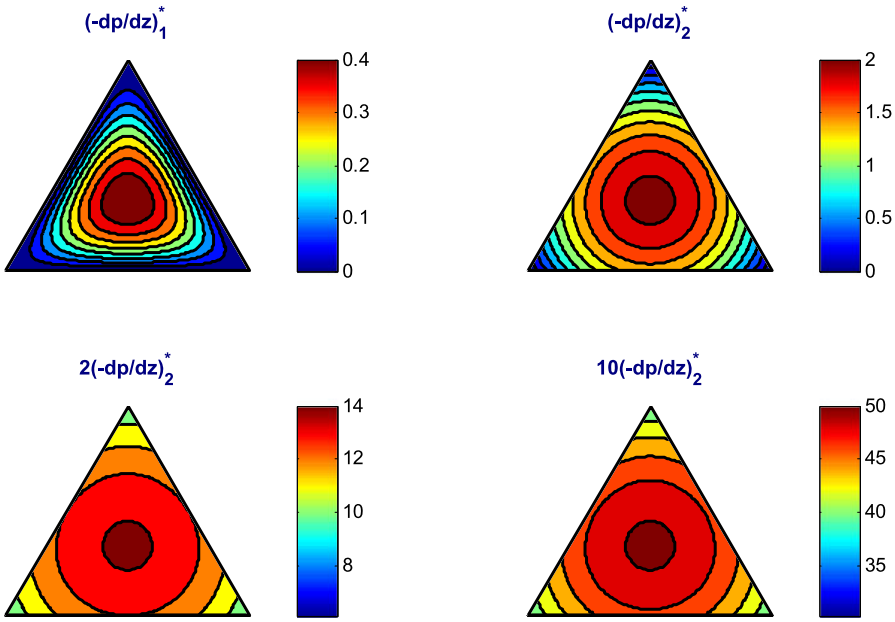

Fig. 6 Velocity contours for $B = 10$ and different values of the dimensionless pressure gradient

flow in this regime not only for triangular ducts but also other geometries is the focus of our current investigations.

Recently, Kalimeris and Fokas [18] presented the solution of several boundary value problems in the interior of an equilateral triangle, including the heat equation with Dirichlet boundary conditions, which is obviously equivalent to solving the time-dependent Poiseuille flow in a triangular duct. An interesting extension of this work may be the solution of start-up

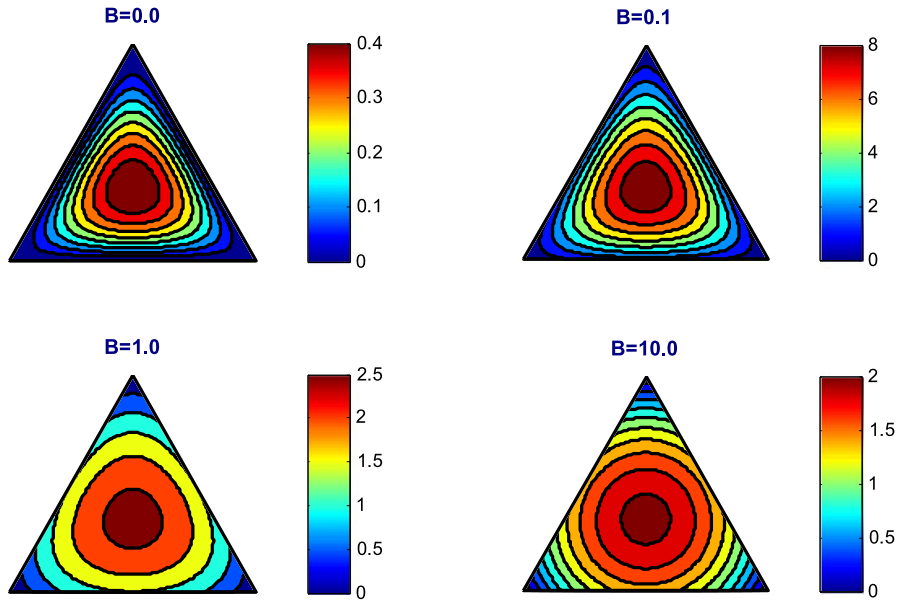

Fig. 7 Velocity contours for different values of B at the second critical pressure gradient $(-\partial p/\partial z)_2^*$. The *top-left graph* ($B = 0$) corresponds to the no-slip case

and cessation of Newtonian Poiseuille flow with slip at the wall.

References

1. Denn MM (2001) Extrusion instabilities and wall slip. Annu Rev Fluid Mech 33:265–287
2. Stone HA, Stroock AD, Ajdari A (2004) Engineering flows in small devices: microfluidics toward a lab-on-a-chip. Annu Rev Fluid Mech 36:381–411
3. Neto C, Evans DR, Bonaccurso E, Butt HJ, Craig VSJ (2005) Boundary slip in Newtonian liquids: a review of experimental studies. Rep Prog Phys 68:2859–2897
4. Hatzikiriakos SG (2012) Wall slip of molten polymers. Prog Polym Sci 37:624–643
5. Navier CLMH (1827) Sur les lois du mouvement des fluides. Mem Acad R Sci Inst Fr 6:389–440
6. Sochi T (2011) Slip at fluid-solid interface. Polym Rev 51:309–340
7. Damianou Y, Georgiou GC, Moulitsas I (2013) Combined effects of compressibility and slip in flows of a Herchel-Bulkley fluid. J Non-Newton Fluid Mech 193:89–102
8. Spikes H, Granick S (2003) Equation for slip of simple liquids at smooth solid surfaces. Langmuir 19:5065–5071
9. Estellé P, Lanos C (2007) Squeeze flow of Bingham fluids under slip with friction boundary condition. Rheol Acta 46:397–404
10. Ballesta P, Petekidis G, Isa L, Poon WCK, Besseling R (2012) Wall slip and flow of concentrated hard-sphere colloidal suspensions. J Rheol 56:1005–1037
11. Ebert WE, Sparrow EM (1965) Slip flow in rectangular and annular ducts. J Basic Eng 87:1018–1024
12. Majdalani J (2008) Exact Navier-Stokes solution for pulsatory viscous channel flow with arbitrary pressure gradient. J Propuls Power 24:1412–1423
13. Wu WH, Wiwatanapataphee B, Hu M (2008) Pressure-driven transient flows of Newtonian fluids through micro-tubes with slip boundary. Physica A 387:5979–5990
14. Wiwatanapataphee B, Wu YH, Hu M, Chayantrakom K (2009) A study of transient flows of Newtonian fluids through micro-annuals with a slip boundary. J Phys A, Math Theor 42:065206
15. Wang CY (2012) Brief review of exact solutions for slip-flow in ducts and channels. J Fluids Eng 134:094501
16. Wang CY (2003) Slip flow in a triangular duct—an exact solution. Z Angew Math Mech 33:629–631
17. Kaoullas G, Georgiou GC (2013) Newtonian Poiseuille flows with wall slip and non-zero slip yield stress. J Non-Newton Fluid Mech 197:24–30
18. Kalimeris K, Fokas AS (2010) The heat equation in the interior of an equilateral triangle. Stud Appl Math 124:283–305